[CANCER RESEARCH 63, 140–148, January 1, 2003]

ERBB2 Up-Regulates *S100A4* and Several other Prometastatic Genes in Medulloblastoma[1]

Roberto Hernan, Rami Fasheh, Christopher Calabrese, Adrian J. Frank, Kirsteen H. Maclean, David Allard, Roger Barraclough, and Richard J. Gilbertson[2]

Departments of Developmental Neurobiology [R. H., R. F., C. C., A. J. F., R. J. G.] and Biochemistry [K. H. M.], St. Jude Children's Research Hospital, Memphis, Tennessee 38105, and School of Biological Sciences, Life Sciences Building, University of Liverpool, Liverpool L69 7ZB, United Kingdom [D. A., R. B.]

ABSTRACT

Medulloblastoma is frequently disseminated throughout the central nervous system by the time of diagnosis. Conventional therapeutic approaches have not reduced the high mortality associated with metastatic medulloblastoma and little is known regarding the molecular mechanisms that promote tumor invasion. Previously, we reported that overexpression of ERBB2 in medulloblastoma is associated with poor prognosis and metastasis. Here, we demonstrate that ERBB2 overexpression increases the migration of medulloblastoma cells across basement membranes *in vitro*. Furthermore, using microarray expression profiling, we show that ERBB2 up-regulates the expression of prometastatic genes in medulloblastoma cells. These include *S100A4*, which was previously shown to promote metastasis of breast cancer. We demonstrate that *S100A4* is a direct target of ERBB2 signaling in medulloblastoma cells via a pathway involving phosphatidylinositol 3-kinase, AKT1, and extracellular signal-regulated kinase 1/2 and that levels of ERBB2 and S100A4 are tightly correlated in samples of primary medulloblastoma. Finally, we show that ERBB2-dependent medulloblastoma cell invasion *in vitro* and prometastatic gene expression *in vivo* can be blocked using the ERBB tyrosine kinase inhibitor OSI-774. These data identify an ERBB2 driven prometastatic pathway that may provide a novel target for therapeutic intervention in metastatic medulloblastoma.

INTRODUCTION

ERBB2 (*HER-2/neu*) signaling through the PI3k[3]/AKT pathway deregulates proliferation (1, 2), impairs apoptosis (3, 4), and increases the metastatic potential of cancer cells (5–15). For example, following activation by ERBB2 and PI3k, AKT phosphorylates the cell cycle inhibitor $p21^{Cip/WAF1}$, which is then relocalized to the cytoplasm, resulting in increased cell proliferation (2). Activated AKT may also induce resistance to DNA-damaging agents in ERBB2 overexpressing cells (3). This appears because of the phosphorylation of MDM2 by AKT, which inhibits the MDM2-$p19^{ARF}$ interaction and promotes p53 degradation. Furthermore, several targets of ERBB2/PI3k signaling have been implicated in tumor angiogenesis and metastasis (12–15). In mouse 3T3 and human MCF-7 breast cancer cells, signaling through this pathway up-regulates expression of vascular endothelial growth factor (15) and enhances cytoskeletal reorganization and tumor cell motility (12–14). As a consequence, overexpression of *ERBB2* is associated with poor prognosis in a number of human cancers (6–8, 16–18).

In addition to ERBB2, several other regulators of metastasis have been proposed to alter the cytoskeleton of tumor cells. These include the calcium binding protein S100A4 (19). Elevated S100A4 expression is correlated with the metastatic potential of tumor cells *in vivo* (20, 21) and with poor clinical outcome in breast and bladder cancer (22, 23). In addition, *S100A4* accelerates metastasis in two independent transgenic models of breast cancer (24, 25).

Previously, we reported that ERBB2 overexpression is associated with poor clinical outcome and advanced metastatic disease stage in medulloblastoma (16, 18, 26, 27). Medulloblastoma is a highly invasive pediatric brain tumor that is frequently disseminated throughout the central nervous system at the time of diagnosis (28). Conventional therapeutic approaches have not reduced the high mortality associated with metastatic medulloblastoma and little is known regarding the molecular mechanisms that promote invasion. Here, we demonstrate that ERBB2 promotes a metastatic phenotype in medulloblastoma by up-regulating a series of pro-metastatic genes, including *S100A4*, and by enhancing tumor cell invasion. We show that ERBB2 directs S100A4 expression via a signaling network that includes PI3k, AKT1, and ERK1/2. Finally, we demonstrate that this prometastatic phenotype can be reversed *in vitro* and *in vivo* using OSI-774 (Erlotinib), a small molecule inhibitor of ERBB2 signaling. Therefore, we identify a new prometastatic pathway that may provide a target for therapeutic intervention in medulloblastoma metastasis.

MATERIALS AND METHODS

Tumor Material. With Institutional Review Board approval, we obtained 51 samples of primary childhood (≤19 years) medulloblastoma from the St. Jude Children's Research Hospital Tumor Bank. Samples were snap frozen at the time of primary surgical resection and stored at −80°C until use. Frozen sections from each sample were examined by light microscopy to ensure ≥80% consisted of tumor. RNA was then extracted from samples by direct homogenization in the TRIzol reagent (Life Technologies, Inc., Gaithersburg, MD).

Cell Culture. We obtained the Daoy medulloblastoma cell line from the American Type Culture Collection. Cells were maintained as monolayer cultures in complete DMEM supplemented with 10% FBS. The effects of small molecule inhibitors on protein expression and *S100A4* promoter activity were performed by culturing Daoy cells for the indicated times in the presence of the appropriate inhibitor (or 0.1% DMSO control) followed by Western blotting and luciferase analysis as described. PD158780, LY249002, and PD98059 were all from Calbiochem-Novabiochem (San Diego, CA). OSI-774 was generously provided by OSI Pharmaceuticals (Melville, NY).

Plasmids. The complete human *ERBB2* cDNA was inserted into the *Hin*dIII site of pcDNA3.1 to generate the construct pcDNA3.1/ERBB2. The first 1487, 1099, 697, and 322 bp of the human *S100A4* promoter region, immediately 5′ of the transcriptional start site, were inserted into the pGL-basic vector to generate plasmids pDA-L47, pDA-L49, pDA-L412, and pDA-L413, respectively. We generated the WT-AKT1 retroviral vector by inserting HA-tagged AKT1 into the *Eco*RI site of the MSCV retroviral vector. DN-AKT1 vectors were similarly prepared using kinase dead K179M or MyrΔ11-60 AKT1 sequences.

Stable Transfections and Retroviral Infections. Daoy cells were transfected with 1 μg of pcDNA3.1 or pcDNA3.1/ERBB2 using the Lipofectamine reagent (Invitrogen Corporation, Carlsbad, CA) and separate clones of *ERBB2*

Received 7/10/02; accepted 10/31/02.

The costs of publication of this article were defrayed in part by the payment of page charges. This article must therefore be hereby marked *advertisement* in accordance with 18 U.S.C. Section 1734 solely to indicate this fact.

[1] This work was supported by Cancer Center Support Grant CA 21765, the American Lebanese Syrian Associated Charities, and grants from the Simon Trory Brain Tumour Fund, the American Brain Tumour Association, the Medical Research Council of the United Kingdom, and the Cancer and Polio Research Fund.

[2] To whom requests for reprints should be addressed, at E-mail: Richard.Gilbertson@stjude.org.

[3] The abbreviations used are: PI3k, phosphatidylinositol 3′-kinase; ERK, extracellular signal-regulated kinase; FBS, fetal bovine serum; HA, Hemagglutinin; WT, wild type; DN, dominant negative; MAPK, mitogen-activated protein kinase; MEK, MAP/ERK kinase; IHC, immunohistochemical; IGFBP5, insulin-like growth factor binding protein-5; STAT, signal transducers and activators of transcription; ERBB TKI, ERBB receptor tyrosine kinase.

(designated Daoy.1–4), and empty vector-transfected (designated Daoy.V) cells selected under G418. Daoy.2 cells were infected with WT-AKT1 or DN-AKT1 retroviral vectors using standard procedures and expression confirmed by HA-specific Western blotting.

Tumor Cell Invasion. The metastatic activity of Daoy.V, Daoy.1, and Daoy.2 cells was measured *in vitro* using the 24-well BD BioCoat FluoroBlok Invasion System as recommended by the manufacturer (BD Biosciences, Bedford, MA). Briefly, 3×10^4 cells were labeled for 20 min with 10 μM of the fluorescent cell probe CellTracker Green (Molecular Probes, Eugene, OR) in 10% FBS DMEM. Cells were then incubated for an additional 30 min in fresh 10% FBS DMEM. Baseline fluorescence analysis confirmed equivalent labeling of the three different Daoy-derived cell types. Ten percent FBS DMEM was then added as a chemoattractant to the lower chambers of the 24-well plates, and cells were seeded into the prehydrated upper wells of the BD BioCoat FluoroBlok chambers. Nonhydrated wells were included as controls. Cells were then cultured under standard conditions for the indicated times and invasion measured from below at excitation wavelength 485 nm and emission wavelength 530 nm using a Fusion Universal Microplate Analyzer (Perkin-Elmer Life Sciences, Boston, MA). The fluorescence of Daoy.1 and 2 cells that had invaded to the undersurface of the membrane was recorded relative to that of Daoy.V cells. Assays were conducted in quadruplicate. The influence of OSI-774 treatment on invasion was performed in an identical fashion using Daoy.2 cells that were preincubated in 30 nM of drug (or 0.1% DMSO only control) for 6 h before labeling with CellTracker Green.

Microarray Expression Analysis. We determined the gene expression profiles of Daoy.V and Daoy.2 cells grown *in vitro* and *in vivo* using Affymetrix microarray analysis. Briefly, first- and second-strand cDNA was synthesized from 5–15 μg of total Daoy cell RNA using the SuperScript Double-Stranded cDNA Synthesis Kit (Life Technologies, Inc., Rockville, MD) and an oligo-dT_{24}-T7 primer. This was then used to prepare cRNA that was labeled with biotinylated UTP and CTP by *in vitro* transcription using a T7 promoter-coupled double-stranded cDNA as template and the T7 RNA Transcript Labeling Kit (ENZO Diagnostics, Inc., Farmingdale, NY). After purification and precipitation at −20°C, 10 μg of this cRNA was fragmented by heat and ion-mediated hydrolysis at 95°C [200 mM Tris-acetate (pH 8.1), 500 mM KOAc, 150 mM MgOAc] and hybridized to the Human Genome U95Av2 oligonucleotide array chip (Affymetrix, Santa Clara, CA). U95Av2 contains 12,600 full-length annotated genes together with additional probe sets designed to represent EST sequences. Arrays were washed at 25°C with 6 × saline-sodium phosphate-EDTA (0.9 M NaCl, 60 mM NaH_2PO_4, 6 mM EDTA +0.01% Tween 20) followed by a stringent wash at 50°C with 100 mM MES, 0.1 M [Na+], 0.01% Tween 20. We then stained arrays with phycoerythrin-conjugated streptavidin (Molecular Probes), and the fluorescence intensities were determined using a laser confocal scanner (Hewlett-Packard, Palo Alto, CA). The scanned images were analyzed using Microarray software (Affymetrix). We standardized for sample loading and variations in staining by scaling the average of the fluorescent intensities of all genes on an array to a constant target intensity (2500) for all arrays used. The expression data were analyzed as described previously (29). The signal intensity for each gene was calculated as the average intensity difference, represented by [Σ (PM − MM)/(number of probe pairs)], where PM and MM denote perfect match and mismatch probes. Separate microarray experiments were conducted for Daoy.V and Daoy.2 clones. We constructed scatterplots comparing the average intensity differences of expression profiles for the two cell types. Genes whose expression significantly varied (positively or negatively ≥2-fold) in Daoy.2 *versus* Daoy.V cells were identified using Spotfire Decision Site 6.2 software (Spotfire, Somerville, MA).

Luciferase Reporter Assay. Daoy.V and Daoy.2 cells were grown to 60–80% confluency and transfected with a 20:1 mix of the pDA *S100A4* and pRL Renilla control luciferase reporter constructs using the Lipofectamine reagent (Invitrogen Corporation). After 48 h, cells were lysed in Passive Lysis Buffer (Promega, Madison, WI) and the firefly (pDA reporter plasmids) relative to *Renilla* (control) luciferase activity determined using the Dual-Luciferase reporter assay (Promega). We assessed the impact of ERBB2, PI3k, and MEK inhibition on the activity of the *S100A4* promoter by repeating these assays in the presence of 5 μM PD158780, 50 μM LY249002, or 50 μM PD98059, respectively.

Western Blotting. Expression of phospho-Y1248 ERBB2 (Upstate Biotechnology, Waltham, MA), phospho-Y204 ERK1/2 (Santa Cruz Biotechnology, Santa Cruz, CA), phospho-Ser473 of AKT1 (New England Biolabs, Beverly, MA), ERBB2 (Novacastra Ltd., Newcastle, United Kingdom), ERK1 (Santa Cruz Biotechnology), AKT1 (New England Biolabs), and S100A4 (Dako, Carpinteria, CA) was performed by Western blotting as previously described (16) using commercially available primary antibodies (companies shown in parentheses). All blots were reprobed with an antibody for β-actin (Sigma Chemicals, St. Louis, MO) to control for protein loading and transfer. We determined the expression level of each protein by densitometric analysis. Expression levels of phospho-specific proteins were normalized to those of the respective total protein.

Northern Blotting. Northern blotting was performed using standard techniques. Briefly, 10 μg of total RNA was separated by formaldehyde gel electrophoresis and transferred to nylon membrane by capillary blotting. Membranes were then probed with a 500-bp, [α^{32}P]dCTP-labeled PCR fragment generated from the COOH-terminal region of the *ERBB2* cDNA. We then stripped and reanalyzed membranes using a probe generated from the entire *S100A4* coding region. Finally, we probed membranes with a PCR-generated fragment of r18S to control for RNA loading and transfer. Expression level of each RNA transcript was determined using Phosphorimaging.

Xenografts and Animal Treatment Protocols. A total of 1×10^7 Daoy.V or Daoy.2 cells was grown as s.c. xenografts in female CD-1 nu/nu mice. When tumors were ~900 mm^3, we euthanized animals and resected tumors. We fixed half of the tumors in 10% buffered formalin and snap froze half in liquid nitrogen. We processed fixed tissue and performed IHC analysis as described previously (16). We extracted total RNA and protein from frozen tissue and performed Western blotting analysis as described above. For therapeutic studies, we treated tumor-bearing mice p.o. with 100 mg/kg (0.1 ml/10 g body weight) of the ERBB tyrosine kinase inhibitor OSI-774 or vehicle only twice daily for 5 days followed by tumor excision and analysis.

RESULTS

ERBB2 Overexpression Up-Regulates the Metastatic Phenotype of Medulloblastoma Cells *in Vitro*. To study the impact of ERBB2 overexpression on the metastatic phenotype of medulloblastoma, we generated clonal derivatives of the Daoy medulloblastoma cell line that express elevated levels of exogenous *ERBB2* (Fig. 1). As previously reported in other cell line systems (30–32), overexpression of ERBB2 in Daoy cells resulted in spontaneous receptor activation and signaling, secondary to receptor homodimerization (Fig. 1 and data not shown).

First, we measured the impact of ERBB2 expression level on Daoy cell migration through basement membranes *in vitro*. Migration of control cells transfected with empty vector alone was readily detected using the BioCoat FluoroBlok Invasion System (BD Biosciences). This is compatible with a recent report that the Daoy cell line is derived from metastatic medulloblastoma (33). However, transfection with *ERBB2* moderately but significantly increased the rate of Daoy cell migration through basement membranes relative to empty vector control cells ($P < 0.05$, Fig. 1*A*).

Overexpression of ERBB2 in human and mouse mammary cancer has been shown to up-regulate a number of important prometastatic genes (34–36). Therefore, we next investigated whether ERBB2 overexpression similarly alters gene expression patterns in Daoy cells. The Daoy cell line is a valid model for studying gene expression in medulloblastoma because the global DNA methylation pattern (37) and basal gene expression profile (33) of this cell line are closely related to those of primary medulloblastoma. Paired expression profiles from four independent cultures of Daoy.2 and Daoy.V cells were compared using the Human Genome U95Av2 Affymetrix microarray containing 12,600 probe sets (Fig. 1*B*). Using scatter plot analysis, we identified 11 genes that significantly differed (≥ or ≤2-fold) in all four comparisons (Fig. 1*B*). As expected, *ERBB2* was among the up-regulated genes. The remaining 10 genes have previously been associated with tumor progression and metastasis (Fig. 1*B*). In a

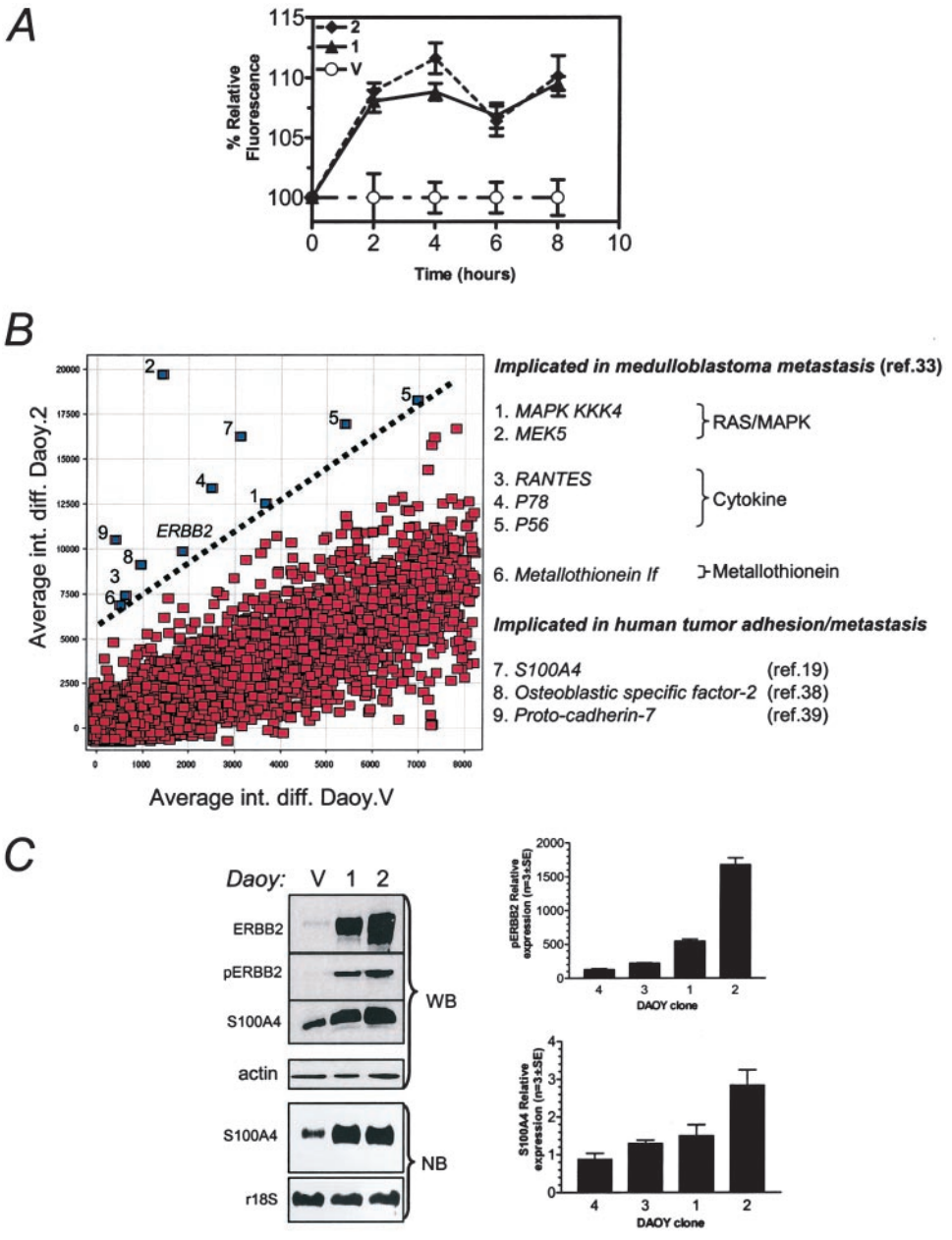

Fig. 1. ERBB2 accelerates the metastatic phenotype in Daoy medulloblastoma cells. *A*, the metastatic phenotype of Daoy cells transfected with empty vector (Daoy.V) or *ERBB2* (Daoy.1 and Daoy.2) was assessed *in vitro* using the BD BioCoat FluoroBlok Invasion System (see "Materials and Methods"). Note ERBB2 overexpression significantly increased Daoy cell invasion and migration relative to empty vector control cells. ($P < 0.05$ for both Daoy.1 and 2 relative to Daoy.V at all time points from 2 to 8 h). *B*, gene expression profiles for Daoy.2 and Daoy.V cells were determined using the Affymetrix U95Av2 microarray. Average intensity difference expression scores for each sequence were compared for the two cell types by scatterplot analysis. The results of one representative comparison are shown in the figure. Assays were conducted in quadruplicate. Genes that were reproducibly and significantly (≥2-fold) up-regulated in Daoy.2 relative to Daoy.V cells are shown as *blue boxes above the dotted line*. These genes are identified on the right of the scatterplot. Note, six genes belong to three groups previously implicated in medulloblastoma metastasis. *C*, ERBB2 and S100A4 mRNA and protein expression are correlated in Daoy cells. The figure shows the results of Western blotting (WB) analyses of total and phospho(Y1248)-ERBB2 and S100A4 expression in Daoy.V, Daoy.1, and Daoy.2 cells. Northern blotting (NB) analysis of S100A4 transcript levels in these cells is shown beneath. Graphs on the right hand side of the figure show the expression of phosphorylated-(p) ERBB2 (*top*) and S100A4 (*bottom*) in four *ERBB2*-transfected Daoy clones (Daoy.1–4) relative to empty vector control cells. Note the correlation between clone expression level of ERBB2 and S100A4 protein.

recent Affymetrix array study of primary medulloblastoma, MacDonald *et al.* (33) reported increased expression of several RAS/MAPK and cytokine signal pathway members and the *metallothionein* family to predict for metastatic medulloblastoma. Interestingly, six of the genes up-regulated by ERBB2 in Daoy cells are also members of these three groups of genes. The three remaining up-regulated genes included *S100A4* (19), *osteoblastic specific factor-2* (also known as *Periostin*; Ref. 38), and *Proto-cadherin-7* (39). Each of these has previously been implicated in controlling cell adhesion and invasion in adult cancers. Finally, one gene, *IGFBP5*, was reproducibly down-regulated by ERBB2 overexpression in Daoy cells. High concentrations of IGFBP5 have been reported to inhibit proliferation of neuroblastoma cells in culture (40).

The novel finding that *S100A4* is up-regulated by ERBB2 in Daoy cells is of particular interest because this gene has been suggested to function as a regulator of metastasis of human tumors in which ERBB2 plays a prominent role (19). Therefore, we further investigated the relationship between ERBB2 and S100A4 in Daoy cells (Fig. 1*C*). In agreement with the results of expression profiling, both S100A4 protein and mRNA levels were higher in Daoy cells transfected with *ERBB2* relative to empty vector. Taken together, these data indicate that overexpression of ERBB2 increases the metastatic phenotype of medulloblastoma cells by increasing invasion and specifically up-regulating the expression of prometastatic genes that include *S100A4*.

High Levels of ERBB2 Correlate with Metastasis and with the Level of S100A4 in Primary Human Medulloblastoma. To establish whether expression levels of ERBB2 and S100A4 are correlated in clinical medulloblastoma, we studied a large cohort of primary tumors using northern blotting (Fig. 2, *A* and *B*). In keeping with our observations in the Daoy cell line, expression levels of ERBB2 and S100A4 were closely correlated in patient samples ($r^2 = 0.67$, $P < 0.0001$). Furthermore, in agreement with our previous studies (9), significantly higher levels of ERBB2 were expressed in metastatic (M_3) compared with localized medulloblastoma (Fig. 2*C*, $P < 0.05$). Together with our *in vitro* studies, these data support the hypothesis

that ERBB2 signaling is prometastatic in primary human medulloblastoma and up-regulates expression of *S100A4*.

The S100A4 Promoter Contains an ERBB2 Response Element. Although synergism between ERBB2 and S100A4 has been shown to promote metastasis of mammary cancer (24), it is not known whether ERBB2 signaling controls S100A4 expression. Therefore, we linked sequences from the first 1487 bp of the human *S100A4* promoter to the pGL luciferase reporter construct to determine whether ERBB2 directly affects *S100A4* transcription in Daoy cells (Fig. 3*A*). The pDA-L47 construct, which includes the first 1487 bp 5′ of the *S100A4* transcription start site, demonstrated 40-fold greater activity in Daoy.2 compared with empty vector control cells (Fig. 3*B*). In contrast, significantly reduced activity was associated with constructs in which bp −1487 to −1099 were deleted (Fig. 3*B*). Therefore, the human *S100A4* promoter likely contains an ERBB2 response element 1099–1487 bp upstream of the transcription start site. Additional studies are under way to identify potential transcription factor binding sites within this region.

ERBB2 Controls S100A4 Expression through a Signaling Pathway Involving PI3K, AKT1, and ERK. Overexpression of ERBB2 in Daoy cells enhances ERK1/2 and AKT1, but not c-Jun NH_2-terminal kinase, p38, STAT3 or STAT5 signaling.[4] Therefore, we assessed the impact of augmenting or inhibiting ERK1/2 and AKT1 activity on the expression and promoter activity of *S100A4* in Daoy.2 cells (Fig. 4). As expected, treatment with the ERBB tyrosine kinase inhibitor PD158780 significantly reduced the phosphorylation of ERBB2, AKT1, and ERK1/2 and inhibited both *S100A4* expression and promoter activity (Fig. 4, *A* and *B*). We next treated Daoy.2 cells with specific inhibitors of MEK1 (PD98059) and PI3k (LY249002) activity. These also abrogated *S100A4* expression and promoter activity. In addition to decreasing AKT1 phosphorylation, PI3k blockade also significantly reduced ERK1/2 phosphorylation. This observation was confirmed using Wortmannin, a second inhibitor of PI3k (data not shown). These data are in agreement with previously published reports that the RAF/MEK/ERK signal cassette is regulated by PI3k/AKT (41, 42).

Finally, to address the role of AKT1 signaling in the control of S100A4 expression, we augmented or reduced its activity in Daoy.2 cells by overexpressing WT-AKT1 and DN-AKT1 constructs, respectively, by transduction with retroviruses overexpressing these proteins. WT-AKT1 markedly decreased ERK1/2 phosphorylation, S100A4 expression, and *S100A4* promoter activity (Fig. 4, *A* and *B*). In contrast, kinase dead K179M-AKT1 significantly increased *S100A4* promoter activity and expression. Infection of cells with MyrΔ11-60 AKT1 also significantly up-regulated S100A4 expression and promoter activity (data not shown).

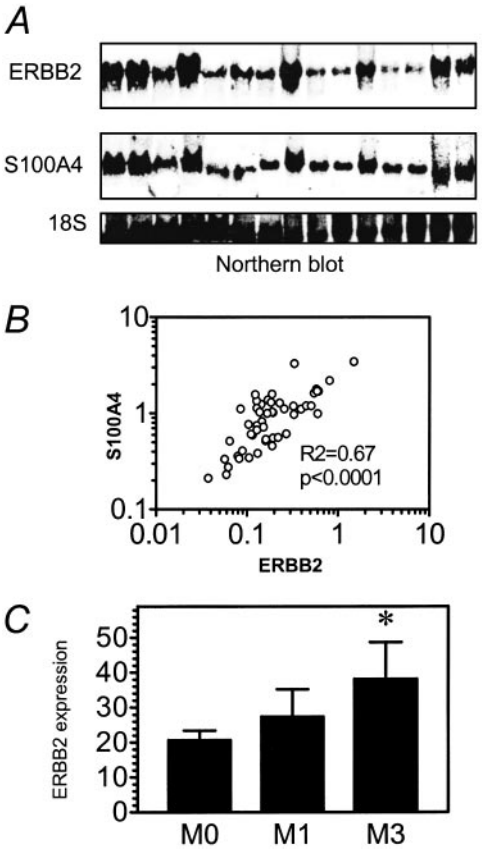

Fig. 2. ERBB2 expression level is correlated with S100A4 expression level and metastatic disease stage in samples of primary human medulloblastoma. *A*, Northern blot analysis of ERBB2 and S100A4 expression in 15 representative samples from a total of 51 analyzed primary medulloblastoma. r18S loading and transfer control blot is shown below. *B*, graph depicts the significant correlation between ERBB2 and S100A4 transcript levels determined by Northern blot analysis in all 51 medulloblastoma samples. Levels were determined by phosphorimager analysis and normalized to r18S control. *C*, graph showing the mean (±SE) ERBB2 transcript expression level for the 51 patient samples grouped by metastatic stage. The mean ERBB2 expression levels for patients with M_0, M_1, and M_3 disease were 20.7 ± 2.7 (n = 28), 27.4 ± 7.8 (n = 9), and 38.1 ± 10.1 (n = 14), respectively. The difference in expression level between M_0 and M_3 disease was statistically significant (*$P < 0.05$).

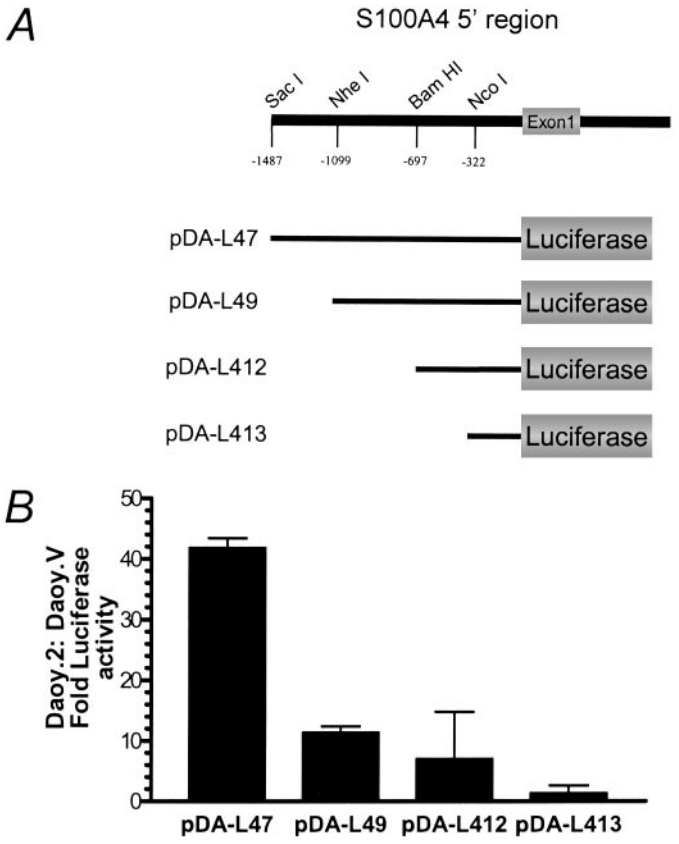

Fig. 3. The human *S100A4* promoter region contains an ERBB2 signal response element. *A*, reporter plasmids used to assay *S100A4* promoter activity in Daoy cells. Cartoon depicting the promoter region of human *S100A4* and restriction sites (*top*) used to generate the four pDA luciferase reporter plasmids (*bottom*). *B*, fold luciferase activity driven by the pDA *S100A4* reporter plasmids in Daoy.2 relative to Daoy.V cells. Assays were conducted in quadruplicate.

[4] C. Calabrese, A. Frank, K. Maclean, Richard Gilbertson. Medulloblastoma sensitivity to 17-allylamino 17-demethoxygeldanamycin requires MEK/ERK, submitted for publication.

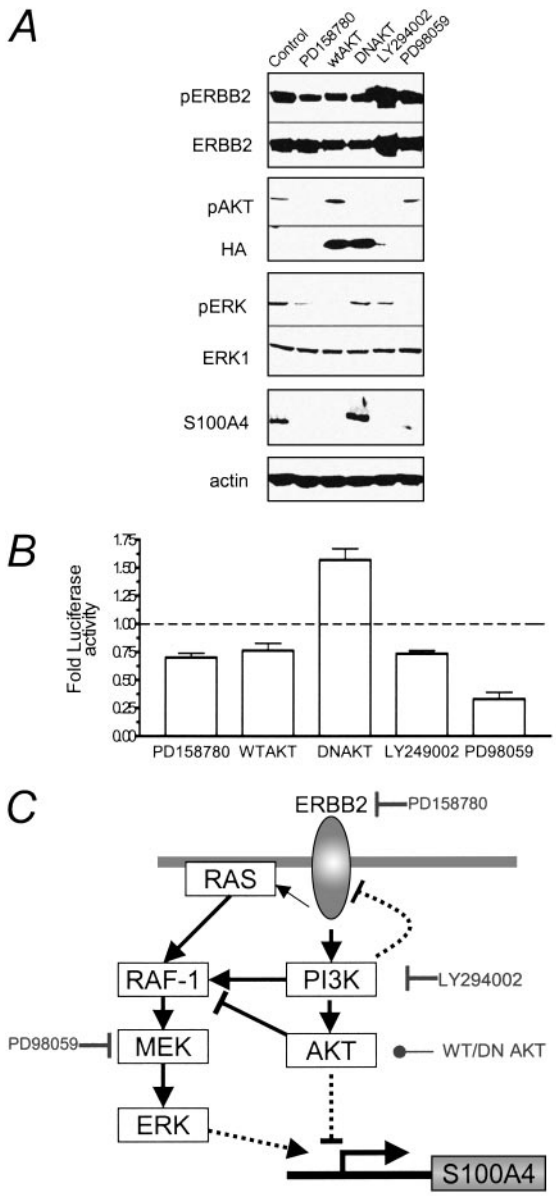

Fig. 4. ERBB2/PI3k signaling controls expression of S100A4 by positively and negatively regulating ERK. *A*, Daoy.2 cells were treated with DMSO only (control), pharmacological inhibitors of the ERBB tyrosine kinase (PD158780), PI3k (LY249002), MEK1 (PD98059), or infected with WT-AKT1 or kinase dead K179M-AKT1 constructs. The impact of these treatments on ERBB2 receptor and second messenger activation status and S100A4 protein expression were determined by phospho-specific and total protein Western blots, respectively. Expression from retroviral infections was confirmed using a HA-specific antibody. *B*, *S100A4* reporter activity parallels the response of total S100A4 protein expression after second messenger inhibitor treatment or AKT1 retroviral infection of Daoy.2 cells. *S100A4* promoter activity was assessed by dual luciferase analysis. Fold promoter activity is shown for each treatment relative to vehicle only-treated Daoy.2 cells. *Bars* denote mean ± SE for triplicate experiments. *C*, cartoon illustrating the proposed interaction between PI3k, AKT1, and ERK1/2 in the control of ERBB2-mediated S100A4 expression. The inhibition of RAF-1 by AKT1 was reported elsewhere (41, 42). Sites of action of chemical and genetic reagents used to elucidate the pathway are shown.

Taken together, these data indicate that ERBB2 signaling via PI3k and ERK1/2 increases expression of S100A4 in Daoy medulloblastoma cells (Fig. 4*C*). Conversely, AKT1 appears to negatively regulate this signal, possibly by inhibiting ERK1/2 activation.

The ERBB Tyrosine Kinase Inhibitor OSI-774 Inhibits the Metastatic Phenotype in Daoy Cells *in Vitro* and *in Vivo*. ERBB2 is central to the pathogenesis of a number of human cancers, therefore many novel agents that target this receptor are currently under development (8, 43). These include small molecule inhibitors of the ERBB TKIs. The ERBB TKIs that are most advanced in clinical development are designed to target ERBB1, *e.g.*, ZD1839 (Iressa) and OSI-774 (Erlotinib). However, there is increasing evidence that these agents may also inhibit ERBB2 signaling (44). Therefore, we investigated the ability of OSI-774 to inhibit ERBB2-directed medulloblastoma cell migration and prometastatic gene expression.

OSI-774 significantly inhibited ERBB2 phosphorylation and S100A4 expression in Daoy cells a time- and dose-dependent manner (Fig. 5*A*). No apparent effect of OSI-774 treatment on ERBB2 activation or S100A4 expression was seen before 4 h. Subsequently, a gradual decrease in the level of phosphorylated ERBB2 was observed in a dose-dependent fashion. This effect was maximal at 8 h. As expected, the inhibition and recovery of ERBB2 phosphorylation was paralleled by changes in S100A4 expression (Fig. 5*A*). We next investigated the ability of OSI-774 to inhibit ERBB2-directed tumor cell invasion. To ensure that ERBB2 receptor signaling was effec-

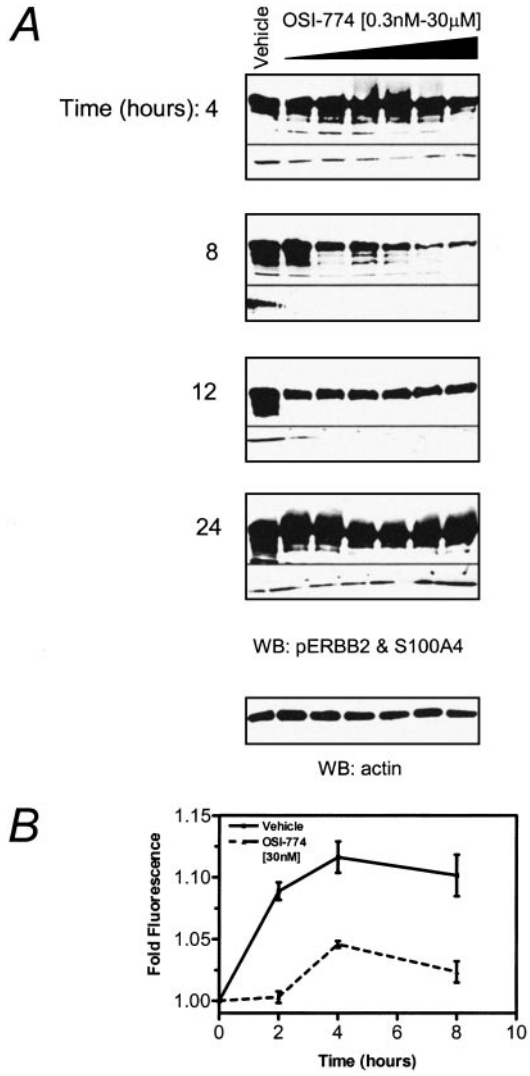

Fig. 5. The ERBB tyrosine kinase inhibitor OSI-774 inhibits ERBB2 phosphorylation, S100A4 expression, and Daoy cell invasion and migration *in vitro*. *A*, Daoy.2 cells were cultured for the times indicated in the presence of DMSO (vehicle) or increasing concentrations of OSI-774. Cells were lysed, and the phosphorylation of ERBB2 determined by Western blotting (WB; *top of each panel*). The same blots were reprobed for S100A4 (*bottom panels*). The actin blot corresponding to 8-h treatment is shown at the *bottom* of the figure. *B*, Daoy.2 cells were preincubated for 6 h with 30 nM OSI-774 or vehicle only and *in vitro* migration measured using the BD BioCoat FluoroBlok Invasion System (see "Materials and Methods"). Note, OSI-774 significantly decreased Daoy.2 cell invasion and migration relative to vehicle-treated control cells ($P < 0.005$).

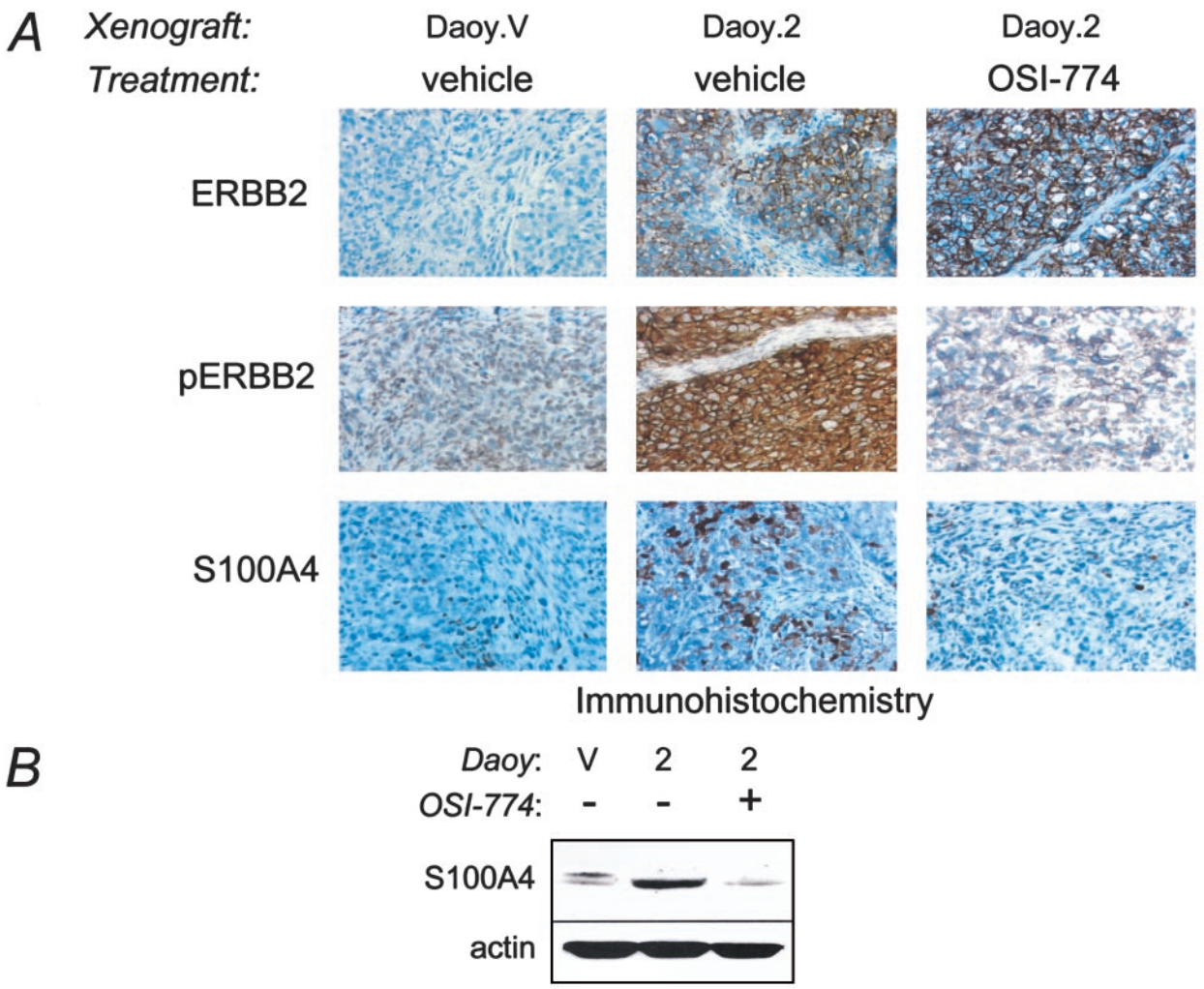

Fig. 6. The oral ERBB TKI OSI-774 selectively inhibits ERBB2 driven gene expression *in vivo*. *A*, IHC analysis of total and phospho-ERBB2 and S100A4 expression by Daoy.V and Daoy.2 xenografts in animals treated with vehicle only or the oral ERBB TKI OSI-774. Treatment with the inhibitor significantly reduced both the phosphorylation status of ERBB2 within xenografts and their expression of S100A4. *B*, Western blot analysis of S100A4 expression by Daoy.V and Daoy.2 xenografts in animals treated with vehicle only (−) or the oral ERBB TKI OSI-774 (+).

tively but specifically inhibited, we preincubated Daoy.2 cells for 6 h with the minimum concentration of drug required to generate receptor blockade (30 nM). This treatment significantly inhibited the migration of Daoy.2 cells *in vitro* (Fig. 5*B*).

Finally, we investigated the ability of OSI-774 to inhibit ERBB2 directed prometastatic gene expression in Daoy.2 cells grown as s.c. xenografts in nude mice. On the basis of our *in vitro* data, we dosed animals every 12 h for 5 days to ensure constant ERBB2 receptor blockade. Western blot and IHC analysis confirmed that Daoy.2 xenografts express much higher levels of total and phospho-ERBB2 and S100A4 than Daoy control tumors (Fig. 6*A*). However, oral dosing of Daoy.2 tumor-bearing animals with OSI-774 markedly reduced the level of phospho-ERBB2 and S100A4 expression by xenografts (Fig. 6, *A* and *B*). Therefore, the control of S100A4 expression by ERBB2 is functionally active *in vivo* and can be effectively targeted with small molecule inhibitors of ERBB2 signaling.

We next extended these analyses to investigate the impact of ERBB2 signaling and blockade on the expression of all nine prometastatic genes that were up-regulated by ERBB2 in culture (Fig. 1*B*). Affymetrix gene expression profiling of xenografts demonstrated that five of these nine genes were also up-regulated by ERBB2 *in vivo* (Table 1). In agreement with our IHC and Western blotting studies (Fig. 6), these included *S100A4*. We next compared the gene expression-profiles of Daoy.2 tumors derived from mice treated with OSI-774 or vehicle alone (Table 1). Only the five genes that were up-regulated by ERBB2 in xenografts were significantly down-regulated by treating host animals with OSI-774. Therefore, up-regulation of prometastatic genes by ERBB2 *in vivo* can be selectively inhibited using an oral small molecule inhibitor of ERBB2 signaling.

DISCUSSION

Metastasis is the leading cause of treatment failure and the most significant predictor of poor clinical outcome in children with medulloblastoma (28, 45). Previously, we reported a significant association between elevated expression of the *ERBB2* oncogene and metastasis in medulloblastoma. Here, we confirmed this association in a separate cohort of 51 pediatric medulloblastomas and demonstrate that ERBB2 signaling increases the metastatic phenotype of medulloblastoma cells by up-regulating expression of prometastatic genes and by increasing tumor cell invasion. Furthermore, we show that this phenotype can be reversed using a small molecule inhibitor of the ERBB2 tyrosine kinase. Therefore, we identify a new prometastatic signaling pathway that may provide a novel target for therapeutic intervention in metastatic medulloblastoma.

Table 1 *Impact of ERBB2 expression and inhibition on the gene expression profile of Daoy xenografts*

The expression of the 10 genes deregulated by ERBB2 overexpression in Daoy cells in culture was investigated *in vivo* using Affymetrix array analysis of Daoy.V and Daoy.2 xenografts. The first column lists the gene names. The second column indicates the mean (±SE) fold difference in expression of each gene between Daoy.2 versus Daoy.V xenografts from three independent experiments. Genes whose expression was significantly up-regulated by ERBB2 overexpression are shown above the dotted line. The third column compares the expression of each gene in Daoy.2 xenografts taken from animals treated with oral OSI-774 (100 mg/kg/twice a day) *versus* vehicle only. Note, only genes whose expression was significantly up-regulated by ERBB2 overexpression were down-regulated by the ERBB2 inhibitor.

	Daoy.2:Daoy.V		Daoy.2 + OSI-774:Daoy.2	
	Fold (±SE)	*P*	Fold (±SE)	*P*
Gene				
OSF-2	224.6 (±1.1)	<0.0001	0.66 (±0.04)	0.001
S100A4	3.11 (±0.14)	0.006	0.75 (±0.01)	0.008
RANTES	2.10 (±0.27)	0.01	0.46 (±0.06)	0.02
p78	1.36 (±0.06)	0.02	0.38 (±0.11)	0.01
p56	1.26 (±0.01)	<0.0001	0.55 (±0.04)	0.005
Metallothionein If	1.01 (±0.6)	NS	1.38 (±0.26)	NS
MAPK KKK4	1.10 (±0.12)	NS	1.14 (±0.16)	NS
MEK5	0.97 (±0.35)	NS	0.94 (±0.10)	NS
PCDH7	0.82 (±0.08)	NS	0.91 (±0.06)	NS
IGFBP5	0.88 (±0.03)	NS	0.99 (±0.20)	NS

The molecular mechanisms responsible for metastasis of medulloblastoma are largely unknown. Recently, members of the RAS/MAPK and cytokine signal pathways and the metallothionein family were identified as predictors of medulloblastoma metastasis (33). In this study, we demonstrate that 6 of 10 genes identified as up-regulated by ERBB2 in cultured medulloblastoma cells also belong to these three groups of genes. Therefore, we propose that these genes are key regulators of medulloblastoma metastasis and that ERBB2 signaling promotes their expression during metastasis.

There is increasing evidence that the cytokine network, including the chemokine group of chemoattractant cytokines, contributes to human tumor growth and progression (46–48). Chemokines released by solid tumors recruit monocytes and macrophages, which in turn secrete a number of tumor cell growth factors, angiogenic growth factors, and extracellular matrix-degrading enzymes (47, 48). Tumor infiltration by monocytes and macrophages is frequently seen in solid tumors, including medulloblastoma (49), and is associated with a poor clinical outcome in certain adult cancers (47, 48). In this study, we show that expression of the CC chemokine *RANTES* and the IFN-inducible genes *p56* and *p78* are up-regulated by ERBB2 in Daoy cells. RANTES is a T cell and monocyte attractant that is produced by several tumors, including carcinomas of the breast and ovary (50, 51). Recent evidence was presented implicating RANTES in promoting angiogenesis and the production of matrix metalloproteinase 9 by monocytes (50). Additional analyses will be required to establish the precise role of cytokine signaling in medulloblastoma metastasis and whether this may be targeted therapeutically.

Metallothionein If was also up-regulated by ERBB2 overexpression in Daoy cells. The metallothioneins, which are preferentially overexpressed in metastatic medulloblastoma and other poor prognosis human tumors (33, 52), are involved in many cellular processes, including metal homeostasis and detoxification, cell proliferation, and apoptosis (53, 54). The metallothioneins may play a permissive role in metastasis by promoting tumor cell resistance to chemotherapeutic agents (53, 54). However, it remains to be determined whether they play a more direct role in invasion and migration.

We also identified four ERBB2-regulated genes that have previously been implicated in controlling cell adhesion and invasion but not medulloblastoma metastasis. These include *osteoblastic specific factor-2* (55) and *PCDH7* (39) that encode cell adhesion molecules, *IGFBP5* (40) and *S100A4* (19). Although S100A4 has been shown to synergize with ERBB2 in the development of metastatic breast cancer (19, 22, 24, 25), it was not know whether ERBB2 signaling directly controls the expression of *S100A4*. Our data show that ERBB2 signaling via PI3k and ERK1/2 does activate *S100A4* expression, at least in part, by enhancing transcription. We also show that the expression of ERBB2 and S100A4 are strictly concordant in primary human medulloblastoma samples and medulloblastoma xenografts, demonstrating that this pathway is active *in vivo*. The observation that ERBB2 up-regulates the expression of two members of the RAS/MAPK pathway (*MAPK KKK4* and *MEK5*) as well as directing *S100A4* expression via this pathway is intriguing. These data suggest that ERBB2 may promote the metastasis of medulloblastoma through a complex series of collaborating events in which this receptor up-regulates both the expression of prometastatic genes, *e.g.*, *S100A4*, and the signal pathways required to do this. Our analyses of the *S100A4* promoter region indicate that ERBB2 signaling controls the expression of this gene via a response element located between bp −1487 and −1099. *Cis*-acting response elements have been identified within the *S100A4* gene. These include a composite enhancer element within the first intron (56) and a GC-factor recognition sequence located 1300 bp upstream of the rodent *S100A4* transcriptional start site (57). We are therefore investigating whether this later sequence coordinates the ERBB2 signaling response. Our data also show that ERBB2/PI3k signaling may abrogate S100A4 expression through interaction between AKT1 and the MEK/ERK pathway. Interaction between these pathways has been described in a number of cell signal systems, including the glial cell line-derived neurotrophic factor signaling system in neuroectodermal cells (42). Therefore, interplay between the ERK1/2 and PI3k systems may be of general importance in neuroectodermal cell growth factor signaling.

Selective targeting of the molecular abnormalities responsible for medulloblastoma metastasis may represent a more effective and less toxic means of treatment than conventional chemo- and radiotherapies. Here, we provide proof of principal that small molecule inhibitors of ERBB2 tyrosine kinase activity may be used to inhibit the prometastatic phenotype in medulloblastoma. Furthermore, our comparative expression profile analyses of tumors resected from OSI-774 and vehicle only-treated animals provide the first evidence to date that these inhibitors selectively reduce the expression of ERBB2 up-regulated genes. Therefore, we propose ERBB2 to be a new therapeutic target for metastatic medulloblastoma. We are currently conducting additional preclinical studies of the antitumor and antimetastatic properties of ERBB2 inhibitors against medulloblastoma. Additional analysis of the other prometastatic genes and pathways identified in this study may also provide additional targets for the development of novel therapeutic approaches. In this regard, MacDonald *et al.* (33) recently reported the platelet-derived growth factor receptor signaling system to be up-regulated in metastatic medulloblastoma and demonstrated the ability of selective inhibitors of this pathway to prevent Daoy tumor cell invasion *in vitro*. Combined ERBB2 and platelet-derived growth factor receptor blockade may therefore prove a particularly effective therapeutic strategy for metastatic medulloblastoma. Finally, it will also be important to determine whether ERBB2 signaling controls S100A4 expression in other human cancers, particularly breast cancer, given the significant role identified for both of these proteins in this disease.

ACKNOWLEDGMENTS

We thank staff of the Hartwell Center for Bioinformatics and Biotechnology at St. Jude Children's Research Hospital for outstanding technical assistance and Tom Curran and John Cleveland for critical reading of this manuscript.

REFERENCES

1. Lane, H. A., Beuvink, I., Motoyama, A. B., Daly, J. M., Neve, R. M., and Hynes, N. E. ErbB2 potentiates breast tumor proliferation through modulation of p27(Kip1)-Cdk2 complex formation: receptor overexpression does not determine growth dependency. Mol. Cell. Biol., *20:* 3210–3223, 2000.
2. Zhou, B. P., Liao, Y., Xia, W., Spohn, B., Lee, M. H., and Hung, M. C. Cytoplasmic localization of p21Cip1/WAF1 by Akt-induced phosphorylation in HER-2/neu-overexpressing cells. Nat. Cell Biol., *3:* 245–252, 2001.
3. Zhou, B. P., Liao, Y., Xia, W., Zou, Y., Spohn, B., and Hung, M. C. HER-2/neu induces p53 ubiquitination via Akt-mediated MDM2 phosphorylation. Nat. Cell Biol., *3:* 973–982, 2001.
4. Hudziak, R. M., Lewis, G. D., Shalaby, M. R., Eessalu, T. E., Aggarwal, B. B., Ullrich, A., and Shepard, H. M. Amplified expression of the HER2/ERBB2 oncogene induces resistance to tumor necrosis factor α in NIH 3T3 cells. Proc. Natl. Acad. Sci. USA, *85:* 5102–5106, 1988.
5. Naume, B., Borgen, E., Kvalheim, G., Karesen, R., Qvist, H., Sauer, T., Kumar, T., and Nesland, J. M. Detection of isolated tumor cells in bone marrow in early-stage breast carcinoma patients: comparison with preoperative clinical parameters and primary tumor characteristics. Clin. Cancer Res., *7:* 4122–4129, 2001.
6. Slamon, D. J., Godolphin, W., Jones, L. A., Holt, J. A., Wong, S. G., Keith, D. E., Levin, W. J., Stuart, S. G., Udove, J., Ullrich, A., *et al*. Studies of the HER-2/neu proto-oncogene in human breast and ovarian cancer. Science (Wash. DC), *244:* 707–712, 1989.
7. Slamon, D. J., Clark, G. M., Wong, S. G., Levin, W. J., Ullrich, A., and McGuire, W. L. Human breast cancer: correlation of relapse and survival with amplification of the HER-2/neu oncogene. Science (Wash. DC), *235:* 177–182, 1987.
8. Yarden, Y., and Sliwkowski, M. X. Untangling the ErbB signalling network. Nat. Rev. Mol. Cell Biol., *2:* 127–137, 2001.
9. Gilbertson, R. J., Clifford, S. C., MacMeekin, W., Meekin, W., Wright, C., Perry, R. H., Kelly, P., Pearson, A. D., and Lunec, J. Expression of the ErbB-neuregulin signaling network during human cerebellar development: implications for the biology of medulloblastoma. Cancer Res., *58:* 3932–3941, 1998.
10. Yu, D., Wang, S. S., Dulski, K. M., Tsai, C. M., Nicolson, G. L., and Hung, M. C. c-erbB-2/neu overexpression enhances metastatic potential of human lung cancer cells by induction of metastasis-associated properties. Cancer Res., *54:* 3260–3266, 1994.
11. Yu, D. H., and Hung, M. C. Expression of activated rat neu oncogene is sufficient to induce experimental metastasis in 3T3 cells. Oncogene, *6:* 1991–1996, 1991.
12. Gambaletta, D., Marchetti, A., Benedetti, L., Mercurio, A. M., Sacchi, A., and Falcioni, R. Cooperative signaling between $\alpha(6)\beta(4)$ integrin and ErbB-2 receptor is required to promote phosphatidylinositol 3-kinase-dependent invasion. J. Biol. Chem., *275:* 10604–10610, 2000.
13. Adam, L., Vadlamudi, R., Kondapaka, S. B., Chernoff, J., Mendelsohn, J., and Kumar, R. Heregulin regulates cytoskeletal reorganization and cell migration through the p21-activated kinase-1 via phosphatidylinositol-3 kinase. J. Biol. Chem., *273:* 28238–28246, 1998.
14. Spencer, K. S., Graus-Porta, D., Leng, J., Hynes, N. E., and Klemke, R. L. ErbB2 is necessary for induction of carcinoma cell invasion by ErbB family receptor tyrosine kinases. J. Cell Biol., *148:* 385–397, 2000.
15. Laughner, E., Taghavi, P., Chiles, K., Mahon, P. C., and Semenza, G. L. HER2 (neu) signaling increases the rate of hypoxia-inducible factor 1α (HIF-1α) synthesis: novel mechanism for HIF-1-mediated vascular endothelial growth factor expression. Mol. Cell. Biol., *21:* 3995–4004, 2001.
16. Gilbertson, R. J., Perry, R. H., Kelly, P. J., Pearson, A. D., and Lunec, J. Prognostic significance of HER2 and HER4 coexpression in childhood medulloblastoma. Cancer Res., *57:* 3272–3280, 1997.
17. Gorlick, R., Huvos, A. G., Heller, G., Aledo, A., Beardsley, G. P., Healey, J. H., and Meyers, P. A. Expression of HER2/erbB-2 correlates with survival in osteosarcoma. J. Clin. Oncol., *17:* 2781–2788, 1999.
18. Herms, J. W., Behnke, J., Bergmann, M., Christen, H. J., Kolb, R., Wilkening, M., Markakis, E., Hanefeld, F., and Kretzschmar, H. A. Potential prognostic value of C-erbB-2 expression in medulloblastomas in very young children. J. Pediatr. Hematol. Oncol., *19:* 510–515, 1997.
19. Mazzucchelli, L. Protein S100A4: too long overlooked by pathologists? Am. J. Pathol., *160:* 7–13, 2002.
20. Ebralidze, A., Tulchinsky, E., Grigorian, M., Afanasyeva, A., Senin, V., Revazova, E., and Lukanidin, E. Isolation and characterization of a gene specifically expressed in different metastatic cells and whose deduced gene product has a high degree of homology to a Ca^{2+}-binding protein family. Genes Dev., *3:* 1086–1093, 1989.
21. Levett, D., Flecknell, P. A., Rudland, P. S., Barraclough, R., Neal, D. E., Mellon, J. K., and Davies, B. R. Transfection of S100A4 produces metastatic variants of an orthotopic model of bladder cancer. Am. J. Pathol., *160:* 693–700, 2002.
22. Davies, B. R., O'Donnell, M., Durkan, G. C., Rudland, P. S., Barraclough, R., Neal, D. E., and Mellon, J. K. Expression of S100A4 protein is associated with metastasis and reduced survival in human bladder cancer. J. Pathol., *196:* 292–299, 2002.
23. Rudland, P. S., Platt-Higgins, A., Renshaw, C., West, C. R., Winstanley, J. H., Robertson, L., and Barraclough, R. Prognostic significance of the metastasis-inducing protein S100A4 (p9Ka) in human breast cancer. Cancer Res., *60:* 1595–1603, 2000.
24. Davies, M. P., Rudland, P. S., Robertson, L., Parry, E. W., Jolicoeur, P., and Barraclough, R. Expression of the calcium-binding protein S100A4 (p9Ka) in MMTV-neu transgenic mice induces metastasis of mammary tumours. Oncogene, *13:* 1631–1637, 1996.
25. Ambartsumian, N. S., Grigorian, M. S., Larsen, I. F., Karlstrom, O., Sidenius, N., Rygaard, J., Georgiev, G., and Lukanidin, E. Metastasis of mammary carcinomas in GRS/A hybrid mice transgenic for the *mts1* gene. Oncogene, *13:* 1621–1630, 1996.
26. Gilbertson, R. J., Pearson, A. D., Perry, R. H., Jaros, E., and Kelly, P. J. Prognostic significance of the c-erbB-2 oncogene product in childhood medulloblastoma. Br. J. Cancer, *71:* 473–477, 1995.
27. Gilbertson, R., Wickramasinghe, C., Hernan, R., Balaji, V., Hunt, D., Jones-Wallace, D., Crolla, J., Perry, R., Lunec, J., Pearson, A., and Ellison, D. Clinical and molecular stratification of disease risk in medulloblastoma. Br. J. Cancer, *85:* 705–712, 2001.
28. Packer, R. J. Childhood medulloblastoma: progress and future challenges. Brain Dev., *21:* 75–81, 1999.
29. Lockhart, D. J., Dong, H., Byrne, M. C., Follettie, M. T., Gallo, M. V., Chee, M. S., Mittmann, M., Wang, C., Kobayashi, M., Horton, H., and Brown, E. L. Expression monitoring by hybridization to high-density oligonucleotide arrays. Nat. Biotechnol., *14:* 1675–1680, 1996.
30. Di Fiore, P. P., Pierce, J. H., Kraus, M. H., Segatto, O., King, C. R., and Aaronson, S. A. erbB-2 is a potent oncogene when overexpressed in NIH/3T3 cells. Science (Wash. DC), *237:* 178–182, 1987.
31. Di Marco, E., Pierce, J. H., Knicley, C. L., and Di Fiore, P. P. Transformation of NIH 3T3 cells by overexpression of the normal coding sequence of the rat neu gene. Mol. Cell. Biol., *10:* 3247–3252, 1990.
32. Olayioye, M. A., Neve, R. M., Lane, H. A., and Hynes, N. E. The ErbB signaling network: receptor heterodimerization in development and cancer. EMBO J., *19:* 3159–3167, 2000.
33. MacDonald, T. J., Brown, K. M., LaFleur, B., Peterson, K., Lawlor, C., Chen, Y., Packer, R. J., Cogen, P., and Stephan, D. A. Expression profiling of medulloblastoma: PDGFRA and the RAS/MAPK pathway as therapeutic targets for metastatic disease. Nat. Genet., *29:* 143–152, 2001.
34. Desai, K. V., Xiao, N., Wang, W., Gangi, L., Greene, J., Powell, J. I., Dickson, R., Furth, P., Hunter, K., Kucherlapati, R., Simon, R., Liu, E. T., and Green, J. E. Initiating oncogenic event determines gene expression patterns of human breast cancer models. Proc. Natl. Acad. Sci. USA, *99:* 6967–6972, 2002.
35. Kumar, R., and Yarmand-Bagheri, R. The role of HER2 in angiogenesis. Semin. Oncol., *28:* 27–32, 2001.
36. Bosc, D. G., Goueli, B. S., and Janknecht, R. HER2/Neu-mediated activation of the ETS transcription factor ER81 and its target gene MMP-1. Oncogene, *20:* 6215–6224, 2001.
37. Fruhwald, M. C., O'Dorisio, M. S., Dai, Z., Tanner, S. M., Balster, D. A., Gao, X., Wright, F. A., and Plass, C. Aberrant promoter methylation of previously unidentified target genes is a common abnormality in medulloblastomas: implications for tumor biology and potential clinical utility. Oncogene, *20:* 5033–5042, 2001.
38. Sasaki, H., Auclair, D., Fukai, I., Kiriyama, M., Yamakawa, Y., Fujii, Y., and Chen, L. B. Serum level of the periostin, a homologue of an insect cell adhesion molecule, as a prognostic marker in non-small cell lung carcinomas. Cancer (Phila.), *92:* 843–848, 2001.
39. Yoshida, K., Yoshitomo-Nakagawa, K., Seki, N., Sasaki, M., and Sugano, S. Cloning, expression analysis, and chromosomal localization of BH-protocadherin (PCDH7), a novel member of the cadherin superfamily. Genomics, *49:* 458–461, 1998.
40. Tanno, B., Negroni, A., Vitali, R., Pirozzoli, M. C., Cesi, V., Mancini, C., Calabretta, B., and Raschella, G. Expression of insulin-like growth factor-binding protein 5 in neuroblastoma cells is regulated at the transcriptional level by c-Myb and B-Myb via direct and indirect mechanisms. J. Biol. Chem., *277:* 23172–23180, 2002.
41. Zimmermann, S., and Moelling, K. Phosphorylation and regulation of Raf by Akt (protein kinase B). Science (Wash. DC), *286:* 1741–1744, 1999.
42. Mograbi, B., Bocciardi, R., Bourget, I., Busca, R., Rochet, N., Farahi-Far, D., Juhel, T., and Rossi, B. Glial cell line-derived neurotrophic factor-stimulated phosphatidylinositol 3-kinase and Akt activities exert opposing effects on the ERK pathway: importance for the rescue of neuroectodermic cells. J. Biol. Chem., *276:* 45307–45319, 2001.
43. Slichenmyer, W. J., and Fry, D. W. Anticancer therapy targeting the erbB family of receptor tyrosine kinases. Semin. Oncol., *28:* 67–79, 2001.
44. Moasser, M. M., Basso, A., Averbuch, S. D., and Rosen, N. The tyrosine kinase inhibitor ZD1839 ("Iressa") inhibits HER2-driven signaling and suppresses the growth of HER2-overexpressing tumor cells. Cancer Res., *61:* 7184–7188, 2001.
45. Zeltzer, P. M., Boyett, J. M., Finlay, J. L., Albright, A. L., Rorke, L. B., Milstein, J. M., Allen, J. C., Stevens, K. R., Stanley, P., Li, H., Wisoff, J. H., Geyer, J. R., McGuire-Cullen, P., Stehbens, J. A., Shurin, S. B., and Packer, R. J. Metastasis stage, adjuvant treatment, and residual tumor are prognostic factors for medulloblastoma in children: conclusions from the Children's Cancer Group 921 randomized Phase III study. J. Clin. Oncol., *17:* 832–845, 1999.
46. Wilson, J., and Balkwill, F. The role of cytokines in the epithelial cancer microenvironment. Semin. Cancer Biol., *12:* 113–120, 2002.
47. Brigati, C., Noonan, D. M., Albini, A., and Benelli, R. Tumors and inflammatory infiltrates: friends or foes? Clin. Exp. Metastasis, *19:* 247–258, 2002.
48. Balkwill, F., and Mantovani, A. Inflammation and cancer: back to Virchow? Lancet, *357:* 539–545, 2001.

49. Rossi, M. L., Buller, J. R., Heath, S. A., Carey, M. P., Carboni, P., Jr., Koutsoubelis, G., and Coakham, H. B. The monocyte/macrophage infiltrate in 35 medulloblastomas: a paraffin-wax study. Tumori, *77:* 36–40, 1991.
50. Azenshtein, E., Luboshits, G., Shina, S., Neumark, E., Shahbazian, D., Weil, M., Wigler, N., Keydar, I., and Ben-Baruch, A. The CC chemokine RANTES in breast carcinoma progression: regulation of expression and potential mechanisms of promalignant activity. Cancer Res., *62:* 1093–1102, 2002.
51. Negus, R. P., Stamp, G. W., Hadley, J., and Balkwill, F. R. Quantitative assessment of the leukocyte infiltrate in ovarian cancer and its relationship to the expression of C-C chemokines. Am. J. Pathol., *150:* 1723–1734, 1997.
52. Janssen, A. M., van Duijn, W., Kubben, F. J., Griffioen, G., Lamers, C. B., van Krieken, J. H., van de Velde, C. J., and Verspaget, H. W. Prognostic significance of metallothionein in human gastrointestinal cancer. Clin. Cancer Res., *8:* 1889–1896, 2002.
53. Jasani, B., and Schmid, K. W. Significance of metallothionein overexpression in human tumours. Histopathology, *31:* 211–214, 1997.
54. Lazo, J. S., Kuo, S. M., Woo, E. S., and Pitt, B. R. The protein thiol metallothionein as an antioxidant and protectant against antineoplastic drugs. Chem. Biol. Interact., *111–112:* 255–262, 1998.
55. Takeshita, S., Kikuno, R., Tezuka, K., and Amann, E. Osteoblast-specific factor 2: cloning of a putative bone adhesion protein with homology with the insect protein fasciclin I. Biochem. J., *294:* 271–278, 1993.
56. Cohn, M. A., Hjelmso, I., Wu, L. C., Guldberg, P., Lukanidin, E. M., and Tulchinsky, E. M. Characterization of Sp1, AP-1, CBF and KRC binding sites and minisatellite DNA as functional elements of the metastasis-associated mts1/S100A4 gene intronic enhancer. Nucleic Acids Res., *29:* 3335–3346, 2001.
57. Chen, D., Davies, M. P., Rudland, P. S., and Barraclough, R. Transcriptional down-regulation of the metastasis-inducing S100A4 (p9Ka) in benign but not in malignant rat mammary epithelial cells by GC-factor. J. Biol. Chem., *272:* 20283–20290, 1997.